DE GRUYTER OPEN

Analele Universităţii de Vest din Timişoara
Vol. LVII, 2013
Seria Fizică

DOI: 10.1515/awutp -2015-0106

THE AHARONOV-BOHM EFFECT AND TRANSPORT PROPERTIES IN GRAPHENE NANOSTRUCTURES

D. Racolta, C. Micu

North University of Baia Mare, Faculty of Science, Str. V. Babes, Nr. 62A, RO-430122, Baia Mare

Article Info
Received: 22.03.2013
Accepted: 05.04.2013

Keywords: Aharonov-Bohm effect, Electronic structure of rapheme, Electronic transport
PACS: 73.23.-b, 73.22.Pr, 72.80.Vp.

Abstract

In this paper we discuss interplays between the Aharonov-Bohm effect and the transport properties in mesoscopic ring structures based on graphene. The interlayer interaction leads to a change of the electronic structure of bilayer graphene ring such that the electronic energy dispersion law exhibits a gap, either by doping one of the layers or by the application of an external perpendicular electric field. Gap adjustments can be done by varying the external electric field, which provides the possibility of obtaining mesoscopic devices based on the electronic properties of bilayer graphene. This opens the way to controllable manipulations of phase-coherent mesoscopic phenomena, as well as to Aharonov-Bohm oscillations depending on the height of the potential step and on the radius of the ring. For this purpose one resorts to a tight-binding model such as used to the description of conductance.

1. Introduction

Transport properties in mesoscopic ring structures based on graphene have received much attention during the last years [1-5]. Graphene (the monolayer graphite) is a recently fabricated material consisting of an individual layer of carbon atoms arranged in a two dimensional hexagonal lattice [1,3]. The honeycomb lattice (Fig.1), provides non-trivial physical phenomena which cannot be observed in the ordinary square lattice [6].

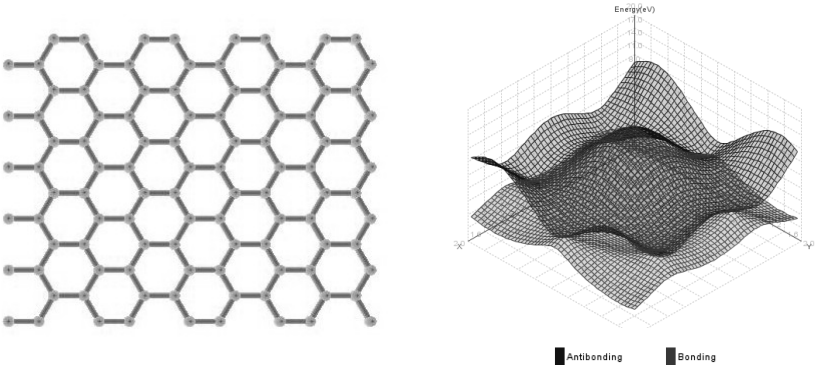

Fig.1.Band structure of graphene. Data are given by:
length=10, width=10, C-C bond length 1.42A, C-C transfer energy 3.013eV.

The especial electronic and magnetic behavior of graphene is defined by the atomic structure of graphene edges. There are two types of graphene structure, namely zigzag and armchair types. These structures differ according to their orientations and the directions of the edges, as shown in Fig.2. Note that the geometry of the underlying lattice is displayed on the left.

Electrons in graphene behave as 2D Dirac fermions and mimic the dynamics of hyper-relativistic electrons [7]. The electronic, magnetic and transport properties of graphene are strongly dependent of their atomic structure edges and opens the way to the controllable onset of phase-coherent mesoscopic phenomena like quantum interference effects, Aharonov-Bohm oscillations and resonant tunneling [8-10].

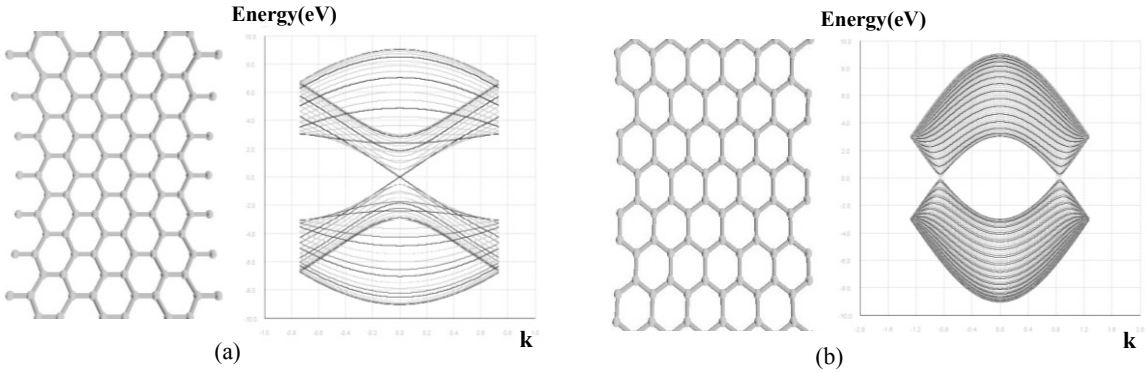

Fig.2. (a) Band structure for arm-chair orientation. Tight binding calculations show that armchair orientation can be semiconducting or metallic depending on width (chirality (m,n)). m=30, n=0, length=10 , C-C bond length 1.42 A and C-C transfer energy 3.013eV. (b) Band structure for zig-zag orientation. Tight-binding calculations show that zigzag orientation is always metallic. m=30, n=30, length=10, C-C bond length 1.42A, C-C transfer energy 3.013eV.

2. Model and formulations

Graphene is also called a „honeycomb lattice" because carbon atoms are arranged in hexagons. The hexagonal lattice is characterized by lattice vectors like $a_1 = \left(\sqrt{3}/2a, a/2\right)$ and, $a_2 = \left(\sqrt{3}/2a, -a/2\right)$where a = 2.46Å.

The calculation of band structure of graphene using tight binding approximation shows that it has semimetal behaviour [11].

The general hopping Hamiltonian of a 2D lattice under the influence of the magnetic field is [12].

$$H = \sum_{i,j} t_{i,j} a_i^+ a_j + H.c., \tag{1}$$

where, $a_j (a_i^+)$ is the annihilation (creation) operator at site *j (i),* H.c. stands for the Hermitian conjugation, whereas $t_{i,j}$ denotes the hopping integral between sites *i* and *j*. The sites *i* and *j* being located in a plan produce a hexagonal square. Diagonalizing the hamiltonian equation and performing the summations yields the wavefunctions of graphene as [11]

$$\psi(k) = -t \exp(ik_x a/\sqrt{3})[1 + 2\exp\left(-ik_x a/\sqrt{3}\right)\cos_y/2] \tag{2}$$

which leads to the eigenvalues

$$E(k) = \pm v_F |k| \tag{3}$$

where $v_F = 3ta/2h$ stands for the Fermi-velocity. Correspondingly, the energy bands derived by virtue of the tight binding Hamiltonian are [11]

$$E(k) = \pm t\sqrt{1 + 4\cos^2\left(\frac{k_y a}{2}\right) + 4\cos\left(\frac{k_y a}{2}\right)\cos\left(\frac{\sqrt{3}k_x a}{2}\right)}. \tag{4}$$

Tight binding model shows, that graphene has full valence band and empty conduction band, while the top of the valence band has exactly the same energy as the bottom of the conduction band. Therefore graphene is called a zero band-gap semiconductor or semimetal, since electronic properties get ranged between the ones of metal and semiconductors. The energy bands of graphene at low energies are described by a *2D* Dirac-like equation with linear dispersion near *K*/*K'*-points in *k* space.

3. Aharonov-Bohm oscillations

The description of Aharonov-Bohm oscillations for the case of hexagonal graphene ring terminated in zigzag edges is based on an extended tight-binding model, now by using a single π-band [13].

The magnetic phase factor is [12-14]

$$\theta_{i,j} = -\frac{2\pi}{\phi_0}\int_i^j \vec{A}\cdot d\vec{l}\ , \tag{5}$$

where, $\vec{A}$ denotes the vector potential associated with the applied perpendicular magnetic field B, $\phi_0 = hc/e$ is the magnetic flux quantum and $dl = \sqrt{dx^2 + dy^2}$. The magnetic flux is given by

$$\Phi = \int \vec{B}\cdot d\vec{S}\,, \tag{6}$$

where the area $S = \pi R^2$, with R being the radius of the *1D* ideal ring. Advances in the measurement of small persistent currents and magnetic moments have also to be mentioned [14]. The Aharonov-Bohm oscillations and the persistent currents are dependent on the magnetic flux Φ, like the case of small mesoscopic metallic rings. Fixing the number of electrons the total magnetization is given by the sum over states as [15]

$$M = -\frac{dE_{tot}}{dB}\,, \tag{7}$$

while the corresponding persistent current is given by [16]

$$I = -c\frac{dE_{tot}}{d\Phi}\,. \tag{8}$$

The total energy

$$E_{tot} = \sum_{i,\sigma}^{occ} \varepsilon_i(B)\,, \tag{9}$$

which concerns non-interacting electrons [17], is given by the sum over all occupied single-particle energies. The index σ runs over spins, as usual. In calculating E_{tot}, only the single-particle tight binding energies for which $\varepsilon_i(B)>0$ are considered [18].

For graphene the levels involving *2s, 2px, 2py* orbitals are either far below or far above the Fermi energy. Accordingly, the conduction and valence band levels right around the Fermi energy (which are responsible for electrical conduction) are essentially formed out of the *2pz* orbitals [19]. This means that the conduction and valence band states can be described quite well by a model that uses only one orbital, i.e. the *2pz* orbital, per carbon atom. This

results in a *(2×2)* matrix , say [*h*(*k*)], which can be written down by summing over unit cells, as well as over the four neighboring unit cells. The matrix element is assumed equal to $-t$ between neighboring carbon atoms and zero otherwise.

The Aharonov Bohm patterns characterizing the magnetization curves exhibit alternately integer *(ϕ_0)* and halved periods *($\phi_0/2$),* as long as the highest occupied state lies wihin the sixfold energy band. The $\phi_0/2$ period reflects the zigzag nature of underlying interior states as shown in Fig.3.

The Aharonov-Bohm effect is a fundamental phenomenon of quantum interference related to the transmission of particles through a closed loop pierced by a magnetic flux. Now we succeeded to prove that one deals with both integer *(hc/e)* and half-integer *(hc/2e)* values for the period of the AB oscillations as a function of the magnetic flux, which complies with the case of mesoscopic metal rings. Odd-even (in the number of Dirac electrons, *N)* parity effects characterized by sawtooth-type patterns have also been discussed before [20-21].

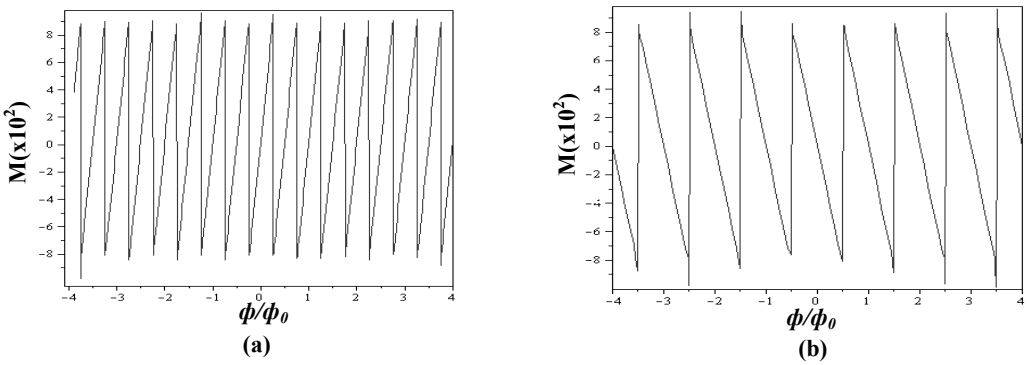

Fig.3. Magnetization as a function of the the magnetic flux ϕ (spin is included). (a) For N = 41one obtains a shifted halved-period sawtooth pattern. (b) For N = 42 one obtains a shifted sawtooth with integer period.

4. Density of states

The study of evolution of the DOS from graphene to a nanotube is based on size quantization effectes which arise as the dimensions are reduced [19]. One starts by establishing the DOS as

$$D(E) = \frac{d}{dE} N(E), \tag{10}$$

where $N(E)$ stands for the total number of electrons. The energy levels can be described by a parabolic dispersion relation with some effective mass m_c:

$$E(k) = E_c + \frac{\hbar^2 k^2}{2m_c}, \tag{11}$$

in which case $d/dE = (dk/dE)d/dk$. Next we have to say that the energy subbands for zigzag nanotubes are given by

$$E(k_x, k_y) \cong E_0 \pm \frac{3ta_0}{2}\sqrt{k_x^2 + \beta_y^2}\,, \tag{12}$$

where,

$$\beta_y = k_y \pm \left(\frac{2\pi}{3b}\right), \quad k_x = \frac{2\pi}{L_x}v_x \quad k_y = \frac{2\pi}{L_y}v_y\,. \tag{13}$$

Further one has

$$\vec{k}\cdot\vec{C} = k_y 2m\pi = 2\pi v \;\;\Rightarrow\;\; k_y = \frac{2\pi}{3b}\frac{3v}{2m}, \tag{14}$$

where the circumferential vector, exhibits an orientation rolling up in y-direction like $(\vec{C} = \hat{y}2bm)$ [19]. Here d is the diameter of the nanotube (nm), so that we have $\pi d = 2mb$ and $C = \pi d = 2\pi m$. It is clear that (12) leads to

$$E(k_x, k_y) \cong E_0 \pm \frac{3ta_0}{2}\sqrt{k_x^2 + \left(k_y - \frac{2\pi}{3b}\right)^2}\,, \tag{15}$$

which can be rewritten as

$$\varepsilon_v(k_x) = E_0 \pm \frac{3ta_0}{2}\sqrt{k_x^2 + k_v^2}\,, \tag{16}$$

where

$$k_v = \frac{2\pi v}{2bm} - \frac{2\pi}{3b} = \frac{2\pi}{2mb}\left(v - \frac{2m}{3}\right). \tag{17}$$

Inserting $k = k_x$, and $\varepsilon = at\sqrt{k^2 + k_v^2}$, one obtains:

$$\frac{d\varepsilon_v}{dk} = at\frac{2k}{2\sqrt{k^2 + k_v^2}} = at\frac{\sqrt{E^2 - a^2t^2k_v^2}}{E}\,, \tag{18}$$

so that

$$\varepsilon^2 - (at)^2 k_v^2 = (at)^2 k^2\,, \tag{19}$$

where $a = 3a_0/2$. In order to obtain the total DOS we have to sum over all subbands

$$D(E) = \sum_v \frac{1}{\pi at}\frac{E}{\sqrt{E^2 - a^2t^2k_v^2}}\,. \tag{20}$$

Then we have to realize that the DOS for zigzag nanotubes with the summation index ν replaced by an integral reads [19]

$$D(E) \approx \int 2dv \frac{2L}{\pi at} \frac{|E|}{\sqrt{E^2 - E_v^2}} \tag{21}$$

In which $dE_v = \frac{2at}{d} dv$. Finally, one finds

$$D(E) = \int_0^E dE_v \frac{2Ld}{\pi a^2 t^2} \frac{|E|}{\sqrt{E^2 - E_v^2}} = \frac{Ld}{a^2 t^2} |E| \tag{22}$$

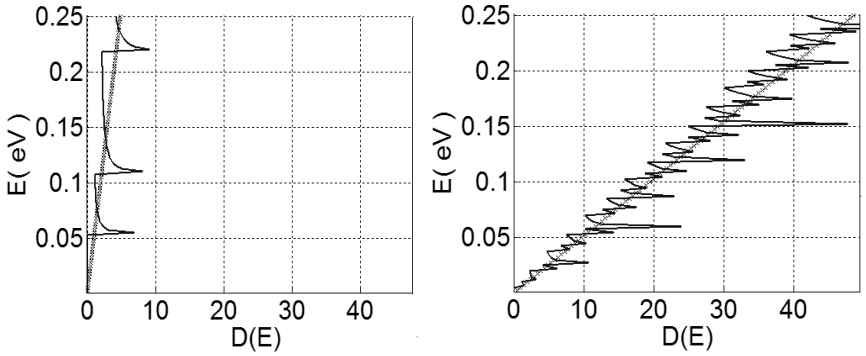

Fig.4. Density of states $D(E)$ for a zigzag nanotube (solid curves) compared with the one of graphite (crosses). (a) m = 100 (corresponding to d = 7.695 nm). (b) m = 1000 (d = 76.96 nm).

It is obvious that in small nanotubes DOS is totally different from graphene, while in larger nanotubes this is less distinctive as shown in Fig.4, especially if we recall that experimental observations are typically convoluted with thermal broadening effects [19]. Recently, experiments using scanning tunneling microscope probes [21], have measured the density of electronic states (DOS), tube diameter, and helicity simultaneously, thereby confirming theoretical predictions.

In addition, sharp peaks in the DOS are observed, which are the characteristic signatures of the one-dimensional (1D) nature of conduction within a 1D system. The 1D nature of the electron system in nanotubes has been observed by resonant Raman scattering experiments, too [23].

5. Conclusions

The electronic structure of nanotubes can be derived from the electronic structure of graphene, by calculating how rolling of the sheet affects the electronic structure. From the periodic boundary conditions of the nanotubes, the wave vector in **C***h* direction becomes quantized, while the wave vector along the nanotubes axis remains continuous. This will

results in a set of *1D* energy dispersion relations which are cross-sections of those for *2D* graphene.

The Aharonov-Bohm effect in graphene rings such as discussed above is a fundamental phenomena for quantum theory and it's important for applications in mesoscopic interferometric devices.

The semiconducting DOS gap depends on the size of a nanotube [19]. Those with small diameters have a large gap and those with large diameters have a small gap. This is especially true at high temperatures, when nanotubes with a large diameter begin to behave like graphene.

References

[1] K. S. Novoselov, A. K. Geim, S. V. Morozov, D. Jiang, Y. Zhang, S. V. Dubonos, I.V. Grigorieva, A. A. Firsov, *Science* **306** (2004) 666.

[2] C. Berger, Z. Song, T. Li, X. Li, A. Y. Ogbazghi, R. Feng, Z. Dai, A. N. Marchenkov, E. H. Conrad, P. N. First, W. A. de Heer, *J. Phys. Chem. B* **108** (2004) 19912.

[3] C. Berger, Z. Song, X. Li, X. Wu, N. Brown, C. Naud, D. Mayou, T. Li, J. Hass, A. N. Marchenkov, E. H. Conrad, P. N. First, W. A. de Heer, *Science* **312** (2006) 1191.

[4] X. Li, X. Wang, L. Zhang, S. Lee, H. Dai, *Science* **319** (2008) 1229.

[5] L. Ci, Z. Xu, L. Wang, W. Gao, F. Ding, K.F. Kelly, B. I. Yakobson, P. M. Ajayan, *Nano Res.* **1** (2008) 116.

[6] Z. Jiang, E. A. Henriksen, L. C. Tung, Y.-J. Wang, M. E. Schwartz, M. Y. Han, P. Kim, and H. L. Stormer, *Phys. Rev. Lett.* **98** (2007) 197403.

[7] C. Neto et al, *Phys World* **105** (2006) 33.

[8] Y. W. Son , M. L. Cohen M L and S. G. Louie, *Phys. Rev. Lett.* **97** (2006) 216803.

[9] M. I. Katsnelson, 2 *Graphene: Carbon in Two Dimensions,* Cambridge University Press (2012).

[10] J. W. González and M. Pacheco, L. Rosales, P. A. Orellana, *Phys. Rev. B* **83** (2011) 155450.

[11] P.R.Wallace, *Physical Review* **71** (1947) 622.

[12] E.Papp, C. Micu, *Low dimensional nanoscale systems on discrete spaces*, World Scientific, Singapore (2007).

[13] J. Schelter, P. Recher, B. Trauzettel, Solid State Communications 152, 1411 (2012).

[14] H. Bluhm, N. C. Koshnick, J. A. Bert, M. E. Huber, K. A. Moler, Phys. Rev. Lett. **102** (2009) 136802.

[15] I. Romanovsky, C. Yannouleas, U. Landman, *Phys. Rev. B* **85** (2012) 165434.

[16] J.T. Chakraborty, P. Pietilainen, *Phys. Rev.B* **50** (1994) 8460.

[17] R. Okuyama, M. Eto, H. Hyuga, *Phys. Rev. B* **83** (2011) 195311.

[18] P. Recher, B. Trauzettel, A. Rycerz, Y. M. Blanter, C.W. J.Beenakker, A. F. Morpurgo, *Phys. Rev. B* **76** (2007) 235404.

[19] S. Datta, *Quantum Transport: Atom to Transistor*, Cambridge University Press, New York, 2005.

[20] H. F. Cheung, Y. Gefen, E. K.Riedel, W. H. Shih, *Phys. Rev.B* **37** (1988) 6050.

[21] E. Papp, C. Micu, L. Aur, D. Racolta, *Physica E* **36** (2007) 178.

[22] J. W. G. Wildoer, L. C. Venema, A. G. Rinzler, R. E. Smalley, C. Dekker, *Nature (London)* **391** (1998) 59.

[23] A. M. Rao, E. Richter, S. Bandow, B. Chase, P. C. Eklund, K. A. Williams, S. Fang, S. Subbaswamy, K. R. Menon, M. Thess, et al. *Science* **275** (1997) 187.